# Analysis and Performance of Waveguide-Hybrid Rings for Microwaves

By H. T. BUDENBOM

This paper presents an analytical treatment of waveguide hybrid rings for microwaves, considered as re-entrant transmission lines. The resulting lines are transformed into equivalent "T" or "lattice" network sections, and determinantal methods are applied in analyzing these equivalent network assemblies for their transmission properties. Some experimental results obtained from a carefully constructed sample of each of two specific types are given. A satisfactory agreement is obtained between the values predicted by theory and experimental results.

## Introduction

IN A recent paper[1], Mr. W. A. Tyrrell has described two general types of waveguide or waveguide/coaxial structures whose properties include bridge or null balance characteristics analogous to those of the hybrid coil common in voice-frequency communication practice. One type, the hybrid junction, is a particular orthogonal junction of four rectangular waveguides. Certain properties of the hybrid junction, notably its impedance characteristics, have been the subject of a British publication[2]. The present paper presents a method for detailed analysis of the other general structure described by Tyrrell, the hybrid ring. This latter structure is essentially an annular ring or annulus of waveguide, at present usually an integral number of quarter wavelengths in circumference, and fitted with an appropriate number of series or shunt branch taps. In this article, phrases such as "quarter wavelength," etc., describing tap spacing or mean annulus perimeter, refer to wavelength in the guide, not to free space wavelength.

The method of analysis employed herein is essentially to treat the tapped annulus as a re-entrant transmission line. Certain circuit equivalences and quarter wave impedance transformations were used by Tyrrell in his paper to develop, with the aid of the reciprocity theorem, many basic properties of hybrid circles and hybrid junctions. In the present paper "T" or "lattice" equivalents (neglecting dissipation) are developed for each section of the annulus, and the method of determinants is applied.

The hybrid junction (known also as the "magic tee") came into use in the newer radars in the latter part of the war. One of its uses, that of providing

[1] "Hybrid Circuits for Microwaves," W. A. Tyrrell, *Proc. I. R. E.*, November 1947.
[2] "The Theory and Experimental Behaviour of Right-Angled Junctions in Rectangular-Section Wave Guides," *I. E. E. Jour.*, September 1946, p. 177.

as outputs the sum and the difference of two input voltages*, is shown on Fig. 1. Matching stubs at the crossing, as indicated, are required to reduce standing waves to a reasonable value. The corresponding type of hybrid ring for providing sum and difference outputs is likewise shown, to-

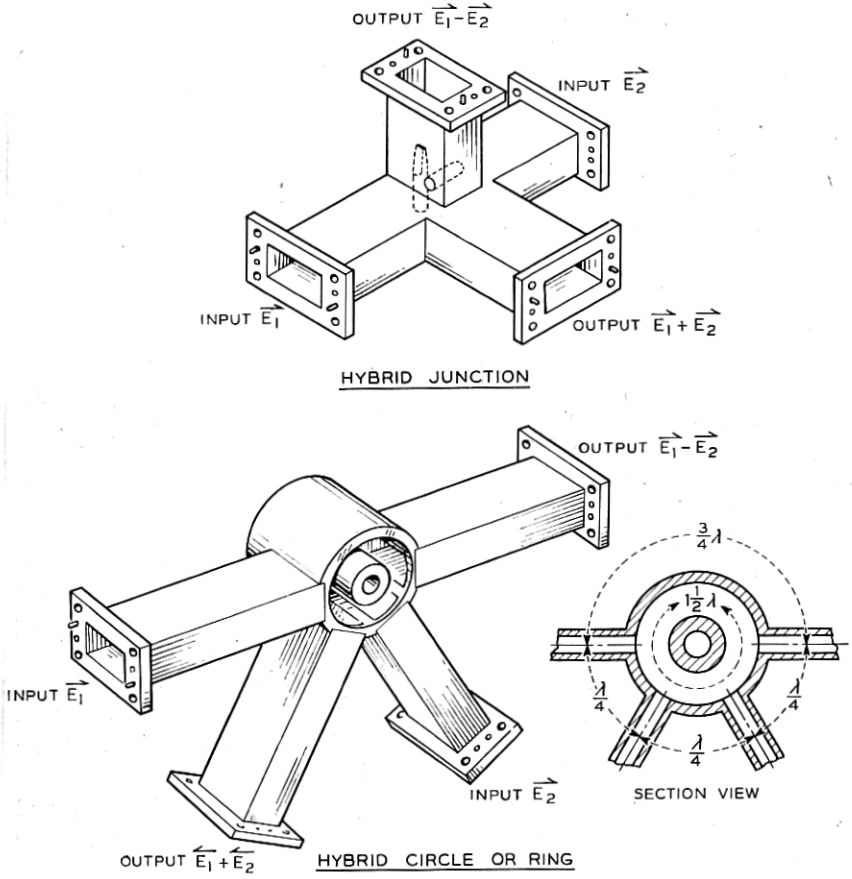


Fig. 1—Hybrid junction and hybrid circle or ring.

gether with a diagram dimensioned in terms of wavelength. Since the path lengths from each input to the output between them are equal, this output gives their sum; the path lengths to the remaining outputs differ by one half wavelength, consequently this output feeds out the difference of the two in-

* More exactly, of two input powers.

puts. No matching stubs are required to achieve a fairly good standing wave ratio; however, the bandwidth over which the ring operates differentially is inherently narrower than that of the junction. The rings have considerably higher power capacity.

The use of hybrids, both junctions and circles, has been noted, as applied to both duplexer and mixer design[3].

There follows a circuit analysis of hybrid rings, primarily of the series type. The method used is to consider the annulus as a continuous line closed on itself. The sections between series taps are then treated as being made up of integral single or multiple quarter wave line sections. Equivalent T or lattice sections are derived for 1, 2, 3, and 4 quarter-wavelength sections, ignoring line dissipation. These equivalences are used to draw equivalent mesh networks. The mesh networks are then solved by determinantal methods. To study some effects of frequency shift off the design center, where the mean periphery of the ring departs from an exact integral number of quarter-wavelengths, the increments in the element values for a quarter-wave equivalent T section are calculated and utilized. The example studied is a ring of $1\frac{1}{2}\ \lambda$ mean perimeter with 3 and 4 taps.

The general procedure neglects possible fringing effects at the junctions. It also neglects the fact that each tap embraces a length of ring which is distinctly more than a small fraction of a wavelength. Nevertheless, the results appear in every case to give a good first approximation. The writer is indebted to Messrs. J. T. Caulfield and J. F. P. Martin for checking the calculations.

Throughout the analysis $Z_0$ represents guide impedance and $\overline{Z}$ represents annulus impedance. It will be noted that the analytical match condition listed is $\sqrt{2}\ \overline{Z} = Z_0$ for the $1\frac{1}{2}\ \lambda$ rings.

The variation of the method necessary to treat the case of shunt taps is indicated.

## I. Circuit Analysis

The rings studied herein are of the series type. This type is the one which results when waveguide is bent in the $H$ plane, into a circle, and tap connections are made to the broad outer face. This type of ring is used, for example, in the "rat race" plumbing.

Such rings may be considered on the basis that the annular slot is a transmission line, whose characteristic impedance will here be called $\overline{Z}$ and propa-

[3] E. G. Schneider, *Proc. I. R. E.*,—August 1946, p. 528 et seq.—see page 550 et seq. and Figs. 40, 42 and 47.

gation constant $P$. The transmission line is closed upon itself. Series connections are made by the waveguide connections. The waveguide outlets are assumed, by virtue of their lengths and/or terminations, to present wave-

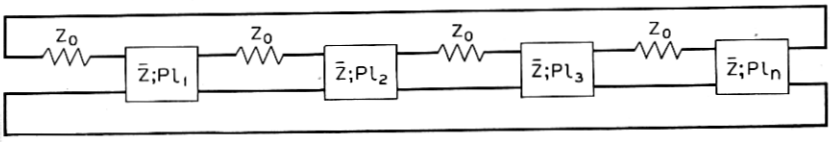


Fig. 2a—Series type hybrid ring as re-entrant transmission line.

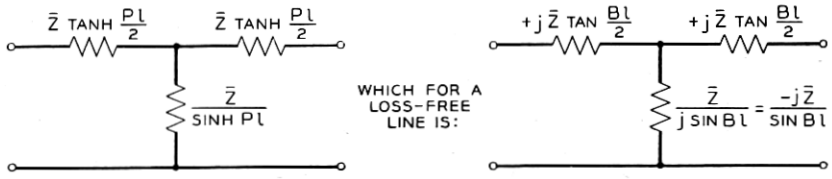


Fig. 2b—T Network equivalent to a line section.

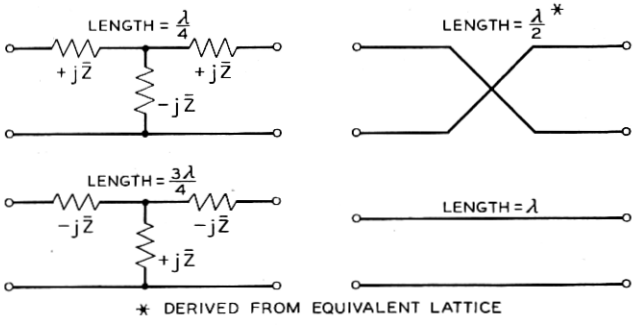


Fig. 2c—Networks equivalent to particular lengths of loss—free line.

* For this case the $T$ becomes indeterminate. However, the needed equivalence can be proved by using the equivalent lattice. If we call $Z_a$ and $Z_b$ the respective series and shunt arms of the $T$, then the equivalent lattice has series arms $= Z_a$ and diagonal arms $Z_a + 2Z_B$ .

guide characteristic impedance to the ring; this will herein be called $Z_0$. Diagrammatically, the situation is as in Fig. 2a. In the course of the following, the line sections will be replaced by equivalent networks, assumed non-dissipative.

## II. Equivalent Line Sections

The first method following evaluates the line sections between outlets. The second views each line section as made up of the necessary number of quarter-wave sections, each represented by its equivalent $T$.

*Method 1*—The equivalent $T$ for a recurrent structure[4] of constants $\bar{Z}$ (characteristic impedance) and $P$ $(=A + jB)$ propagation constant per unit length is as shown in Fig. 2b.

There result the equivalences sketched in Fig. 2c.

Once the circuit is diagrammed using the above equivalences, it can be reduced to simpler form by successive combinations of $Ts$, by well known formulae.

*Method 2*—Determinants. We now consider the line to be made up of the appropriate number of quarter-wave sections, with series taps. Thus we will have Fig. 3.

The shunt impedances are identical; call each $Y$. The series impedances are made identical by first assuming a tap at each quarter-wave junction;

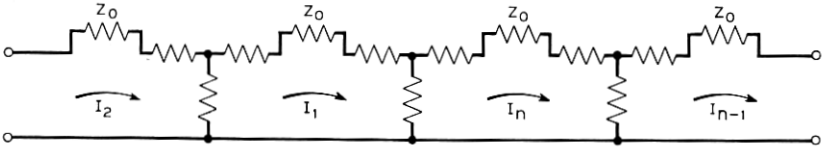


Fig. 3—Re-entrant line as succession of equivalent (quarter wave) T networks and series taps.

call each series leg $S$. Then the (skew symmetrical) circuit determinant for the case where $N = 10$, (or a $2\frac{1}{2}$ wavelength ring) is

$$D_{10} = \begin{vmatrix} (S+2Y) & -Y & 0 & 0 & 0 & 0 & 0 & 0 & 0 & -Y \\ -Y & (S+2Y) & -Y & 0 & 0 & 0 & 0 & 0 & 0 & 0 \\ 0 & -Y & (S+2Y) & -Y & 0 & 0 & 0 & 0 & 0 & 0 \\ 0 & 0 & -Y & (S+2Y) & -Y & 0 & 0 & 0 & 0 & 0 \\ 0 & 0 & 0 & -Y & (S+2Y) & -Y & 0 & 0 & 0 & 0 \\ 0 & 0 & 0 & 0 & -Y & (S+2Y) & -Y & 0 & 0 & 0 \\ 0 & 0 & 0 & 0 & 0 & -Y & (S+2Y) & -Y & 0 & 0 \\ 0 & 0 & 0 & 0 & 0 & 0 & -Y & (S+2Y) & -Y & 0 \\ 0 & 0 & 0 & 0 & 0 & 0 & 0 & -Y & (S+2Y) & -Y \\ -Y & 0 & 0 & 0 & 0 & 0 & 0 & 0 & -Y & (S+2Y) \end{vmatrix} \quad \text{II—2.1}$$

Now, for the case of an exact integral number of quarter wavelengths around the ring, all $Y_{1-n} = -j\bar{Z}$ and all $S_{1-n} = Z_0 + 2j\bar{Z}$, so all $S + 2Y = Z_0$.

[4] K. S. Johnson, "Transmission Circuits for Telephone Communication" Book published by D Van Nostrand Co., New York, N. Y.

The determinant then becomes

$$D'_{10} = \begin{vmatrix} Z_0 & +j\bar{Z} & 0 & 0 & 0 & 0 & 0 & 0 & 0 & +j\bar{Z} & E_1 \\ +j\bar{Z} & Z_0 & +j\bar{Z} & 0 & 0 & 0 & 0 & 0 & 0 & 0 & E_2 \\ 0 & +j\bar{Z} & Z_0 & +j\bar{Z} & 0 & 0 & 0 & 0 & 0 & 0 & E_3 \\ 0 & 0 & +j\bar{Z} & Z_0 & +j\bar{Z} & 0 & 0 & 0 & 0 & 0 & E_4 \\ 0 & 0 & 0 & +j\bar{Z} & Z_0 & +j\bar{Z} & 0 & 0 & 0 & 0 & E_5 \\ 0 & 0 & 0 & 0 & j\bar{Z} & Z_0 & +j\bar{Z} & 0 & 0 & 0 & E_6 \\ 0 & 0 & 0 & 0 & 0 & +j\bar{Z} & Z_0 & +j\bar{Z} & 0 & 0 & E_7 \\ 0 & 0 & 0 & 0 & 0 & 0 & +j\bar{Z} & Z_0 & +j\bar{Z} & 0 & E_8 \\ 0 & 0 & 0 & 0 & 0 & 0 & 0 & +j\bar{Z} & Z_0 & +j\bar{Z} & E_9 \\ +j\bar{Z} & 0 & 0 & 0 & 0 & 0 & 0 & 0 & +j\bar{Z} & Z_0 & E_{10} \end{vmatrix} \quad \text{II—2.2}$$

For a $1\frac{1}{2}\ \lambda$ ring, $n = 6$ and the system shrinks to

$$D_6 = \begin{vmatrix} Z_0 & +j\bar{Z} & 0 & 0 & 0 & +j\bar{Z} \\ +j\bar{Z} & Z_0 & +j\bar{Z} & 0 & 0 & 0 \\ 0 & +j\bar{Z} & Z_0 & +j\bar{Z} & 0 & 0 \\ 0 & 0 & +j\bar{Z} & Z_0 & +j\bar{Z} & 0 \\ 0 & 0 & 0 & +j\bar{Z} & Z_0 & +j\bar{Z} \\ +j\bar{Z} & 0 & 0 & 0 & +j\bar{Z} & Z_0 \end{vmatrix} \quad \text{II—2.3}$$

For the study of the effects occurring if we move off the design center, we can modify the individual $Ts$ to a length $\ell = \frac{\lambda}{4} \pm \frac{\lambda}{N}$. Each series arm, assuming no line dissipation, and $N$ large so $\frac{\lambda}{N} \ll \lambda$, is:

$$j\bar{Z} \tan\left[\frac{2\pi}{\lambda}\left(\frac{\ell}{2}\right)\right] = j\bar{Z} \tan\left[\frac{2\pi}{2\lambda}\left(\frac{\lambda}{4} \pm \frac{\lambda}{N}\right)\right] = j\bar{Z} \tan\left[\frac{\pi}{4} \pm \frac{\pi}{N}\right]$$

$$= j\bar{Z}\,\frac{1 \pm \tan \pi/N}{1 \mp \tan \pi/N} \doteq j\bar{Z}(1 \pm 2\pi/N) = j\bar{Z}(1 \pm \Delta) \quad \text{II—2.4}$$

Similarly, each shunt arm is:

$$\frac{\bar{Z}}{j \sin\left[\frac{2\pi}{\lambda}(\ell)\right]} = \frac{\bar{Z}}{j \sin\left[\frac{2\pi}{\lambda}\left(\frac{\ell}{4} \pm \frac{\lambda}{N}\right)\right]} = \frac{\bar{Z}}{j \sin\left[\frac{\pi}{2} \pm \frac{2\pi}{N}\right]}$$

$$= \frac{-j\bar{Z}}{\sin\frac{\pi}{2}\cos\frac{2\pi}{N}} = \frac{-j\bar{Z}}{\cos\Delta} \doteq \frac{-j\bar{Z}}{1 - \Delta^2/2} \doteq -j\bar{Z}\left(1 + \frac{\Delta^2}{2}\right) \doteq -j\bar{Z} \quad \text{II—2.5}$$

So the shunt arm is, to a first approximation, not affected by a small shift off design center. Our shunts $Y$ thus remain $-j\bar{Z}$ and

$$S + 2Y = Z_0 + 2j\bar{Z} \pm 2j\Delta\bar{Z} - 2j\bar{Z} = Z_0 \pm 2j\Delta\bar{Z}.$$

Therefore, determinants II—2.2 and II—2.3 can be used by merely considering $\overline{Z}_0 + j2\Delta\overline{Z}$ as a special value of $Z_0$.

As is well known,[5,6] the current solutions are obtained by writing in an external column the driving voltages, opposite their associated meshes, as is done at the right of II—2.2. In the present case the number of driving voltages is usually one, never more than two; so the column will be zeros, save for one (or two) meshes. The current in any mesh is a fraction having $D$ as denominator, and as numerator the minor formed from $D$ by substitut-

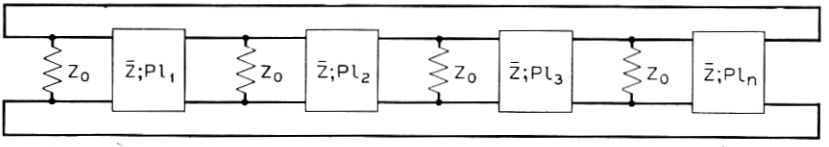


Fig. 4a—Re-entrant line with shunt taps.

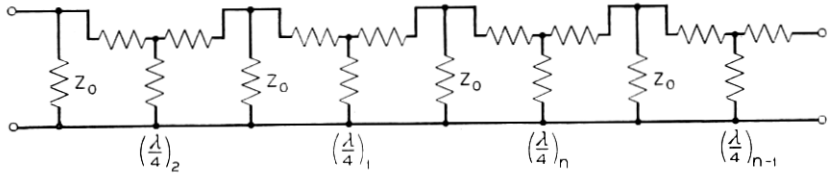


Fig. 4b—Re-entrant line with shunt taps—T networks as line equivalents.

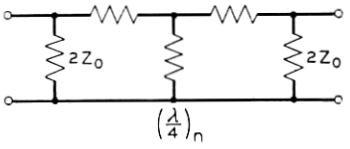


Fig. 4c—Element typical single shunt tapped section.

ing the e.m.f. column in the column corresponding to the mesh where the current is desired, i.e., column $n$ if $I_n$ is desired.

Since $D$ is common to all mesh current expressions, questions of relative power division between branches or of null balance can be handled by operations performed entirely with the numerator minors.

Some slight advantage in evaluating the numerator minors is gained by proceeding where possible so as to make $I_1$ or $I_n$ the desired current.

[5] E. A. Guillemin, "Communication Networks," Vols. I and II. Books published by John Wiley and Sons Inc., New York, N. Y.

[6] L. Silberstein, "Synopsis of Applicable Mathematics." Book published by D. Van Nostrand Co., New York, N. Y.

Alternatively, meshes where $Z_0 = 0$ can be chosen. Another needed quantity is driving point impedance. Since $I_n = \frac{E \cdot d_n}{D}$, then $\frac{1}{Z_{D.P.}} = \frac{d_n}{D}$ and $Z_{DP} = \frac{D}{d_n}$. The resulting impedance will include an extra $Z_0$, the generator impedance, to which we must match.

It may be of interest to show how the reentrant transmission line analysis can be extended to the case of hybrid rings involving shunt taps. For the reiterative shunt case we have the conditions illustrated in Fig. 4a. With substitution of quarter-wave equivalences Fig. 4a becomes Fig. 4b. Clearly determinants analogous to II—2.1 et seq. can be written for this structure. Alternatively we can split each $Z_0$ into two parallel impedances, each $2Z_0$, yielding a typical symmetrical section which can be reduced to a simple $T$ or $\pi$ by well known transformation methods[4] as shown in Fig. 4c.

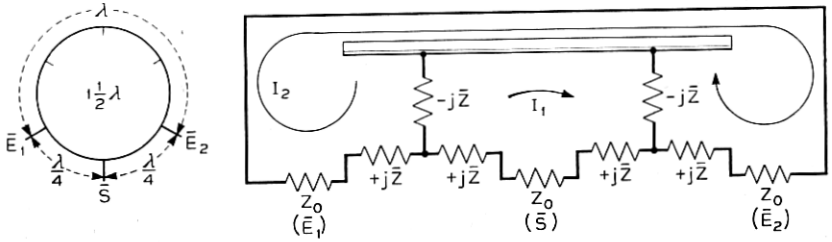


Fig. 5—1½ λ ring—3 arm—equivalent mesh circuit.

## III. Detailed Analysis of Specific Cases of Series Type Rings

*Case A. 1½ λ Ring—3 Arm—As Power Divider—Two Way*

This is most simply analyzed using equivalents from Method 1. The equivalent circuit is shown in Fig. 5. It is immediately clear that:

a. Power fed in at $\bar{S}$ will divide equally between $\bar{E}_1$ and $\bar{E}_2$.

b. Although $\bar{E}_1$ and $\bar{E}_2$ are in proper wavelength relationship for isolation relative to each other, they are effectively in series and there will not be cancellation. The particular wavelength spacing is thus a necessary but not sufficient condition.

c. With a voltage $E$ at $(\bar{S})$ we will have

$$E = I_1 Z_0 - I_2(-2j\bar{Z})$$
$$o = -I_1(-2j\bar{Z}) + I_2(2Z_0)$$

or

$$\begin{vmatrix} E & Z_0 & +2j\bar{Z} \\ o & +2j\bar{Z} & 2Z_0 \end{vmatrix} \qquad \text{III—1}$$

[4] loc. cit. page 282.

so

$$\frac{I_1}{E} = \frac{2Z_0}{2Z_0^2 + 4\bar{Z}^2}$$

and the mesh impedance at $S$ is

$$\frac{Z_0^2 + 2\bar{Z}^2}{Z_0} = Z_0 + \frac{2\bar{Z}^2}{Z_0}.$$

Therefore an impedance match is secured if

$$\sqrt{2}\,\bar{Z} = Z_0. \qquad \text{III—2}$$

d. For a voltage $e$ at $\bar{E}_1$, the current at $\bar{E}_2$ may be obtained from

$$\begin{array}{c|cc} e & 2Z_0 & -2j\bar{Z} \\ o & -2j\bar{Z} & Z_0 \end{array}$$

and is

$$\frac{eZ_0}{2Z_0^2 + 4\bar{Z}^2}. \qquad \text{III—3}$$

Under the impedance match condition $\sqrt{2}\bar{Z} = Z_0$, this is $e/4Z_0$ which is just half the current which could be drawn through a load $Z_0$ connected to a source $Z_0$ with internal voltage $e$. Therefore, the "loss" from $\bar{E}_1$ to $\bar{E}_2$ is 6 db.

*Case B. $1\frac{1}{2}\lambda$ Ring—4 Arms—As Power Divider and Null Device*

*As power divider—Two Way* (Fig. 6). Using the determinantal method, let $\bar{E}_1$ be in mesh 1. Then $D$ is in mesh 4, $\bar{E}_2$ in mesh 5 and $\bar{S}$ in mesh 6. $Z_0 = 0$ for meshes 2 and 3. Then the determinant of II—2.3 and its minor for mesh 5 ($\bar{E}_2$ in Fig. 6) with voltage applied at $\bar{E}_1$, are respectively, from II—2.3:

$$D'_6 = \begin{vmatrix} Z_0 & +j\bar{Z} & 0 & 0 & 0 & j\bar{Z} \\ +j\bar{Z} & 0 & +j\bar{Z} & 0 & 0 & 0 \\ 0 & +j\bar{Z} & 0 & +j\bar{Z} & 0 & 0 \\ 0 & 0 & +j\bar{Z} & Z_0 & +j\bar{Z} & 0 \\ 0 & 0 & 0 & +j\bar{Z} & Z_0 & +j\bar{Z} \\ +j\bar{Z} & 0 & 0 & 0 & +j\bar{Z} & Z_0 \end{vmatrix} \qquad \text{III—3}$$

and

$$d'_5 = \begin{vmatrix} +j\bar{Z} & 0 & +j\bar{Z} & 0 & 0 \\ 0 & +j\bar{Z} & 0 & +j\bar{Z} & 0 \\ 0 & 0 & +j\bar{Z} & Z_0 & 0 \\ 0 & 0 & 0 & +j\bar{Z} & +j\bar{Z} \\ +j\bar{Z} & 0 & 0 & +j\bar{Z} & Z_0 \end{vmatrix} \qquad \text{III—4}$$

Upon expansion $d'_5$ is found to be 0. Therefore, by adding outlet $\bar{D}$, we have isolated branch $\bar{E}_1$ from branch $\bar{E}_2$. (Compare with case A.) Since

it is well known for this structure that $\bar{D}$ is isolated from input at $\bar{S}$, it must follow that an input at $S$ will still divide equally betwen $\bar{E}_1$ and $\bar{E}_2$.

*As Null Device (1½λ—4 Arms).* We now associate $\bar{S}$ with mesh 1, $\bar{E}_1$ with mesh 2, $\bar{D}$ with mesh 5, $\bar{E}_2$ with mesh 6 (see Fig. 7) which leads to:

$$D_6 = \begin{vmatrix} Z_0 & +j\bar{Z} & 0 & 0 & 0 & +j\bar{Z} \\ +j\bar{Z} & Z_0 & +j\bar{Z} & 0 & 0 & 0 \\ 0 & +j\bar{Z} & 0 & +j\bar{Z} & 0 & 0 \\ 0 & 0 & +j\bar{Z} & 0 & +j\bar{Z} & 0 \\ 0 & 0 & 0 & +j\bar{Z} & Z_0 & +j\bar{Z} \\ +j\bar{Z} & 0 & 0 & 0 & +j\bar{Z} & Z_0 \end{vmatrix} \qquad \text{III—3.5}$$

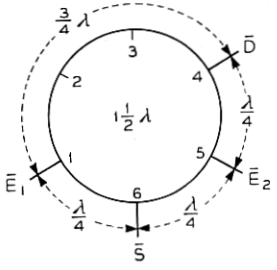


Fig .6

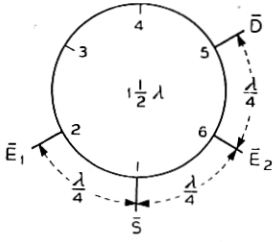


Fig. 7

Fig. 6—1½ λ ring—4 arm—tap spacing and identification for power division analysis by determinants.

Fig. 7—1½ λ ring—4 arm—tap spacing and identification for determinantal analysis as null device.

With voltage applied at $\bar{S}$, mesh 1, the minor for current at $\bar{D}$, mesh 5 is:

$$d_{5(\bar{S})} = + \begin{vmatrix} +j\bar{Z} & Z_0 & +j\bar{Z} & 0 & 0 \\ 0 & +j\bar{Z} & 0 & +j\bar{Z} & 0 \\ 0 & 0 & +j\bar{Z} & 0 & 0 \\ 0 & 0 & 0 & +j\bar{Z} & +j\bar{Z} \\ +j\bar{Z} & 0 & 0 & 0 & Z_0 \end{vmatrix} \qquad \text{III—5.1}$$

where the $5(\bar{S})$ indicates that the voltage is at $\bar{S}$ and the current is sought at mesh 5. Corresponding minors for the current in mesh $5(\bar{D})$, due to voltages at $\bar{E}_1$ and $\bar{E}_2$ are:

$$d_{5(\bar{E}_1)} = - \begin{vmatrix} Z_0 & +j\bar{Z} & 0 & 0 & +j\bar{Z} \\ 0 & +j\bar{Z} & 0 & +j\bar{Z} & 0 \\ 0 & 0 & +j\bar{Z} & 0 & 0 \\ 0 & 0 & 0 & +j\bar{Z} & +j\bar{Z} \\ +j\bar{Z} & 0 & 0 & 0 & Z_0 \end{vmatrix} \qquad \text{III—5.2}$$

$$d_{5(\bar{E}_2)} = - \begin{vmatrix} Z_0 & +j\bar{Z} & 0 & 0 & +j\bar{Z} \\ +j\bar{Z} & Z_0 & +j\bar{Z} & 0 & 0 \\ 0 & +j\bar{Z} & 0 & +j\bar{Z} & 0 \\ 0 & 0 & +j\bar{Z} & 0 & 0 \\ 0 & 0 & 0 & +j\bar{Z} & +j\bar{Z} \end{vmatrix} \qquad \text{III—5.3}$$

Evaluating, we find $d_{5(\bar{S})} = 0$, showing $\bar{D}$ is isolated from $\bar{S}$. The other two expansions give

$$d_{5(\bar{E}_1)} = (+j\bar{Z})[2\bar{Z}^4 - \bar{Z}^2 Z_0^2]$$

and

$$d_{5(\bar{E}_2)} = (+j\bar{Z})[\bar{Z}^2 Z_0^2 - 2\bar{Z}^4]. \qquad \text{III—5.4}$$

So the difference between the voltages at $\bar{E}_1$ and $\bar{E}_2$ is transmitted to $\bar{D}$. Hereafter we will operate on a single voltage at $\bar{S}$. Note, incidentally, that if the $\bar{S}$ arm were not terminated the $Z_0$ in column 1, row 1 of $d_{5(\bar{E}_1)}$ and $d_{5(\bar{E}_2)}$ would be zero, in which case

$$d_{5(\bar{E}_1)} = -(+j\bar{Z})(2\bar{Z}^4) \text{ and } d_{5(\bar{E}_2)} = +(+j\bar{Z})(2\bar{Z}^4) \qquad \text{III—5.5}$$

To study frequency shift on current from $\bar{S}$ at $\bar{D}$ we can write III—5.1 as

$$d_{5(\Delta)} = \begin{vmatrix} +j\bar{Z} & Z_0+2j\Delta\bar{Z} & +j\bar{Z} & 0 & 0 \\ 0 & +j\bar{Z} & 2j\Delta\bar{Z} & +j\bar{Z} & 0 \\ 0 & 0 & +j\bar{Z} & 2j\Delta\bar{Z} & 0 \\ 0 & 0 & 0 & +j\bar{Z} & +j\bar{Z} \\ +j\bar{Z} & 0 & 0 & 0 & Z_0+2j\Delta\bar{Z} \end{vmatrix} \qquad \text{III—6}$$

$$= 2\bar{Z}^2(-\bar{Z}^2 j\Delta\bar{Z} + 2Z_0\Delta\bar{Z}^2 + 4j\Delta\bar{Z}^3) = -2\bar{Z}^4 \cdot \Delta\bar{Z}. \qquad \text{III—7.1}$$

*Match Condition.* The impedance match condition is readily shown to be $\sqrt{2}\bar{Z} = Z_0$ as for the three-arm $1\frac{1}{2}\lambda$ ring.

## Construction of Test Samples

From the drawing of the hybrid circle (Fig. 1), it will be seen that the multiple soldering of guides into the ring can present difficulty in fabrication, especially where numerous branches are required. In addition, early measurements indicated the necessity of accurate dimensions, both linear and angular. As a consequence, the experimental hybrid circles which were used in the measurements reported herein were milled from brass cylinders. Figure 8 shows a 4-branch ring opened so that interior detail can be seen. This form of experimental construction enables dimensions to be held to average values of about half a thousandth of an inch and ten minutes of arc. The mating surfaces are flat to within this tolerance. However, no currents resulting from the field tend to flow in the direction crossing the gap and no loss ensues from this source. These mechanical tolerances are essential only to a basic experiment of the nature here described; larger tolerances could undoubtedly be specified in practice.

## Experimental Results

There follows a tabulation of some experimental data on samples of the specific series types analyzed. The attenuation figures are probably good to ± .25 db up to 10 db, to ± .5 db up to 50 db. The SWR figures may not be better than ± .2 db.

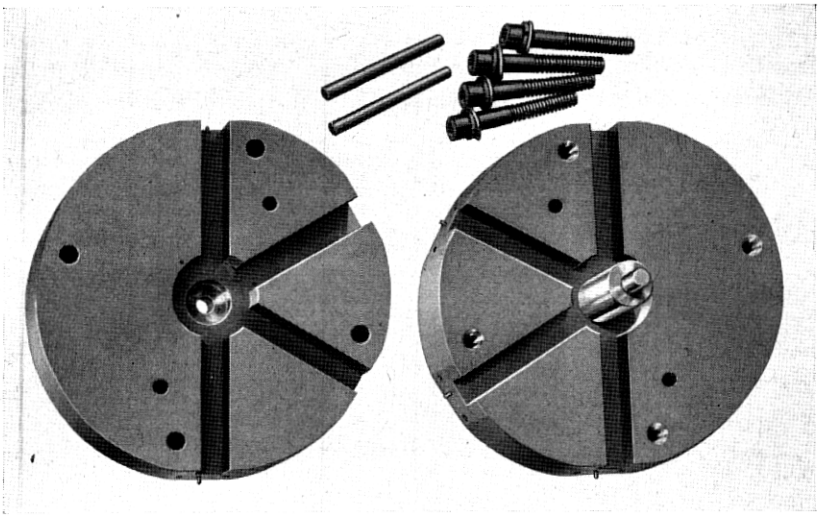

Fig. 8—1½ λ ring—4 arm—photograph of machined test sample.

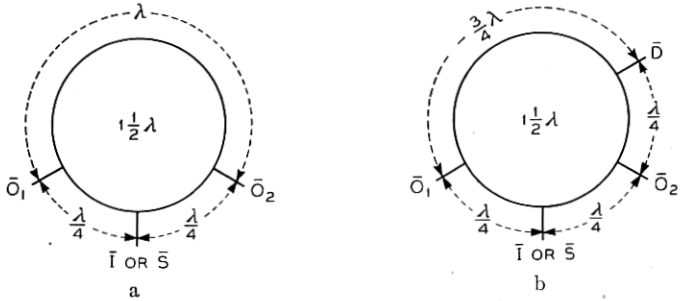


Fig. 9a—1½ λ ring—3 arm—as power divider.
Fig. 9b—1½ λ ring—4 arm—as power divider and null device.

The data are for structures built in terms of .900 inch by .400 inch rectangular guide size (inside) and the test wavelengths* are in the 3-centimeter region. The design wavelength* is $\lambda_0$, the test wavelength $\lambda$*.

*Case A*: 1½λ; Three Arms; Impedance Match $\sqrt{2}\bar{Z} = Z_0$; Reference Fig. 9a:

* These are space wavelengths.

| | Experimental values at % $(\lambda - \lambda_0)/\lambda_0$ | | | | |
|---|---|---|---|---|---|
| | −6% | −3% | 0 | +3% | +6% |
| Power Division. Input at $\bar{I}$. Relative power output at $\bar{O}_1$ or $O_2$ in db (approx. constant over band) | ← | ← | −3.7 ($\bar{O}_1$)<br>−3.5 ($\bar{O}_2$) | → | → |
| Transmission Loss (Isolation) between $\bar{O}_1$ and $\bar{O}_2$ in db (approx. constant over band). $\bar{I}$ terminated. | ← | | 6.0 | | → |
| Standing Wave Ratio (SWR) in db at $\bar{I}$. Outlets $\bar{O}_1$ and $\bar{O}_2$ terminated. | 1.10 | 2.32 | .84 | 1.50 | 1.20 |

*Case B*: $1\frac{1}{2}\lambda$; Four Arms; Impedance Match $\sqrt{2}\bar{Z} = Z_0$; Reference Fig. 9b:

| | Experimental values at $100(\lambda - \lambda_0)/\lambda_0$ | | | | |
|---|---|---|---|---|---|
| | −6% | −3% | 0 | +3% | +6% |
| Power Division. Input at $\bar{I}$. Relative power output at $\bar{O}_1$ or $\bar{O}_2$ in db (approx. constant over band). | ← | ← | −3.5 ($\bar{O}_1$)<br>−3.5 ($\bar{O}_2$) | → | → |
| Transmission Loss (Isolation) between $\bar{O}_1$ and $\bar{O}_2$ in db $\bar{I}$ and $\bar{D}$ terminated. | 20.3 | | 48.5 | | 19.7 |
| Transmission Loss (Isolation) between $\bar{S}$ and $\bar{D}$ in db $\bar{O}_1$ and $\bar{O}_2$ terminated. | 24.0 | | 47.7 | | 22.2 |
| Standing Wave Ratio (SWR) in db at $\bar{I}$ ($\bar{S}$). Outlets at $\bar{O}_1$, $\bar{O}_2$ and $\bar{D}$ terminated. | 3.50 | 1.20 | .66 | .77 | 2.20 |

## Comparison Between Theory and Experiment

From the experimental results, we can now cite in support of the theory the following areas of agreement between theory and experiment, at the design wavelength:

| Ring Type and Property | Theory | Experiment |
|---|---|---|
| *Case A*: $1\frac{1}{2}\lambda$; *Three Arms* | | |
| Relative power at $\bar{O}_1$ and $\bar{O}_2$ for input at $\bar{I}$. | −3 db | −3.6 db |
| Impedance match (SWR) | 0 db | .84 db |
| Observed center wavelength versus mean annulus perimeter guide wavelength | Agreement to about 1% | |
| Transmission loss (Isolation) from $\bar{O}_1$ to $\bar{O}_2$. $\bar{I}$ terminated. | 6.0 db | 6.0 db |
| *Case B*: $1\frac{1}{2}\lambda$; *Four Arms* | | |
| Relative power at $\bar{O}_1$ and $\bar{O}_2$ for input at $\bar{I}$ | −3 db | −3.5 db |
| Impedance Match (SWR) | 0 db | .66 db |
| Transmission Loss (Isolation) $\bar{S}$ to $\bar{D}$. $\bar{O}_1$ and $\bar{O}_2$ terminated | Conjugacy | 47.7 db |
| Transmission Loss (Isolation) $\bar{O}_1$ to $\bar{O}_2$. $\bar{D}$ and $\bar{I}$ terminated | Conjugacy | 48.5 db |

## Conclusion

It is concluded that the theory developed provides calculated results in satisfactory accord with experiment.

It will be recalled that the approximation was initially made that the line sections were loss free. The theory could doubtless be extended to include dissipation by retaining a small real component in the propagation constant $P$ of Fig. 2b. No doubt this real component could, in turn, be included to adequate accuracy in the equivalences of Fig. 2c by the addition of real components in the series arms only. That is, the series arm for a $\lambda/4$ section would be $\bar{Z}\,(r + j1) = r\,\bar{Z} + j\,\bar{Z}$ where $r \ll 1$. Since such terms appear as part of the $(S + 2\,Y)$'s in the basic determinant II—1, which is the same as in series with the $Z_0$'s in determinant II—2, the inclusion of dissipation would appear to be formally straightforward.